

P.J.G. Teunissen and P.F. de Bakker

Abstract

In this contribution we study the multi-frequency, carrier-phase slip detection capabilities of a single receiver. Our analysis is based on an analytical expression that we present for the multi-frequency minimal detectable carrier phase cycle slip.

Keywords

GNSS Cycle Slips • Minimal Detectable Bias (MDB) • Multi-Frequency Receivers

1 Introduction

In this contribution we will study the Global Navigation Satellite System (GNSS) reliability of multi-frequency single-receiver, single-satellite code- and carrier phase time series. Examples of such studies for the single-baseline GNSS models can be found in [Teunissen \(1998\)](#), [De Jong \(2000\)](#), [De Jong and Teunissen \(2000\)](#). There are several advantages to single-receiver, single-satellite data validation. First, it can be executed in real-time inside the receiver and thus enables early quality control on the raw data. Second, the geometry-free single-satellite approach has the advantage that no satellite positions need to be known beforehand and thus no complete navigation

messages need to be read and used. Moreover, this approach also makes the method very flexible for processing data from any (future) GNSS in a simple way, like e.g. (modernized) GPS (USA), Galileo (EU), Glonass (Russia), and Compass (China).

Our study of the single-receiver, single-satellite reliability will be analytical and supported with numerical results. As reliability measure we focus on the Minimal Detectable Biases (MDBs). The MDB is a measure for the size of model errors that can be detected with a certain power and a certain probability of false alarm. The MDB can be determined from the functional and stochastic model and is therefore a useful tool to assess how well certain model errors can be detected. We formulate alternative hypotheses for model errors like outliers in the code data on different frequencies, cycle slips in the carrier phase data on different frequencies, potential loss of lock, and ionospheric disturbances. The closed form formulas that will be presented are applicable to any GNSS with an arbitrary number of frequencies and include also the ionosphere-weighted case. Due to lack of space, we only work out the single- and multi-frequency MDBs for cycle slips. However, the same approach can be followed for the other type of model errors as well.

P.J.G. Teunissen (✉)
Delft Institute of Earth Observation and Space Systems, Delft
University of Technology, Delft, The Netherlands

Department of Spatial Sciences, Curtin University
of Technology, Perth, Australia
e-mail: p.j.g.teunissen@tudelft.nl

P.F. de Bakker
Delft Institute of Earth Observation and Space Systems, Delft
University of Technology, Delft, The Netherlands

We emphasize the results for (modernized) GPS and Galileo.

2 The Multi-frequency Single-Receiver Geometry-Free Model

Null Hypothesis: The carrier phase and pseudo range observation equations of a single receiver that tracks a single satellite on frequency f_j ($j = 1, \dots, n$) at time instant t ($t = 1, \dots, k$), see e.g., [Teunissen and Kleusberg \(1998\)](#), [Misra and Enge \(2001\)](#), [Hofmann-Wellenhoff and Lichtenegger \(2001\)](#), [Leick \(2003\)](#), are given as

$$\begin{aligned}\phi_j(t) &= \rho^*(t) - \mu_j \mathcal{I}(t) + b_{\phi_j} + n_{\phi_j}(t) \\ p_j(t) &= \rho^*(t) + \mu_j \mathcal{I}(t) + b_{p_j} + n_{p_j}(t)\end{aligned}\quad (24.1)$$

where $\phi_j(t)$ and $p_j(t)$ denote the observed carrier phase and pseudo range, respectively, with corresponding zero mean noise terms $n_{\phi_j}(t)$ and $n_{p_j}(t)$. The unknown parameters are $\rho^*(t)$, $\mathcal{I}(t)$, b_{ϕ_j} and b_{p_j} . The lumped parameter $\rho^*(t) = \rho(t) + c\delta t_r(t) - c\delta t^s(t) + T(t)$ is formed from the receiver-satellite range $\rho(t)$, the receiver and satellite clock errors, $c\delta t_r(t)$ and $c\delta t^s(t)$, respectively, and the tropospheric delay $T(t)$. The parameter $\mathcal{I}(t)$ denotes the ionospheric delay expressed in units of range with respect to the *first* frequency. Thus for the f_j -frequency pseudo range observable its coefficient is given as $\mu_j = f_1^2/f_j^2$. The parameters b_{ϕ_j} and b_{p_j} are the phase bias and the instrumental code delay, respectively. The phase bias is the sum of the initial phase, the phase ambiguity and the instrumental phase delay.

Both b_{ϕ_j} and b_{p_j} are assumed to be time-invariant. This is allowed for relatively short time spans, in which the instrumental delays remain sufficiently constant. The time-invariance of b_{ϕ_j} and b_{p_j} implies that only time-differences of $\rho^*(t)$ and $\mathcal{I}(t)$ are estimable. We may therefore just as well formulate the observation equations in time-differenced form. Then the parameters b_{ϕ_j} and b_{p_j} get eliminated and we obtain

$$\begin{aligned}\phi_j(t, s) &= \rho^*(t, s) - \mu_j \mathcal{I}(t, s) + n_{\phi_j}(t, s) \\ p_j(t, s) &= \rho^*(t, s) + \mu_j \mathcal{I}(t, s) + n_{p_j}(t, s)\end{aligned}\quad (24.2)$$

where $\phi_j(t, s) = \phi_j(t) - \phi_j(s)$, with a similar notation for the time-difference of the other variates.

Would we have a priori information available about the ionospheric delays, we could model this through the use of additional observation equations. In our case, we do not assume information about the *absolute* ionospheric delays, but rather on the *relative*, time-differenced, ionospheric delays. We therefore have the additional (pseudo) observation equation

$$\mathcal{I}_o(t, s) = \mathcal{I}(t, s) + n_{\mathcal{I}_o}(t, s) \quad (24.3)$$

with the (pseudo) ionospheric observable $\mathcal{I}_o(t, s)$. The sample value of $\mathcal{I}_o(t, s)$ is usually taken to be zero.

If we define $\phi(t) = (\phi_1(t), \dots, \phi_n(t))^T$, $p(t) = (p_1(t), \dots, p_n(t))^T$, $y(t) = (\phi(t)^T, p(t)^T, \mathcal{I}_o(t))^T$, $g(t) = (\rho^*(t), \mathcal{I}(t))^T$, $\mu = (\mu_1, \dots, \mu_n)^T$, $y(t, s) = y(t) - y(s)$ and $g(t, s) = g(t) - g(s)$, then the expectation $E(\cdot)$ of the $2n + 1$ observation equations of (24.2) and (24.3) can be written in the compact vector-matrix form

$$E(y(t, s)) = Gg(t, s) \quad (24.4)$$

where

$$G = \begin{bmatrix} e_n & -\mu \\ e_n & +\mu \\ 0 & 1 \end{bmatrix} \quad (24.5)$$

This two-epoch model can be extended to an arbitrary number of epochs. Let $y = (y(1)^T, \dots, y(k)^T)^T$ and $g = (g(1)^T, \dots, g(k)^T)^T$, and let D_k be a full rank $k \times (k - 1)$ matrix of which the columns span the orthogonal complement of e_k , $D_k^T e_k = 0$ (recall that e_k is a k -vector of 1's). Then $\Delta y = (D_k^T \otimes I_{2n+1})y$ and $\Delta g = (D_k^T \otimes I_2)g$ are the time-differenced vectors of the observables and parameters, respectively, and the k -epoch version of (24.4) can be written as

$$\mathcal{H}_0 : E(\Delta y) = (I_{k-1} \otimes G)\Delta g \quad (24.6)$$

where \otimes denotes the Kronecker product. Model (24.6), or its two-epoch variant (24.4), will be referred to as our null hypothesis \mathcal{H}_0 .

Alternative Hypotheses: The data collected by a single GNSS receiver can be corrupted by many different errors. The errors that we consider are the ones that can be modelled as a shift in the mean of

the data vector, $E(\Delta y | \mathcal{H}_a) = E(\Delta y | \mathcal{H}_0) + \text{shift}$. Modelling errors of this kind are outliers in the pseudo range data, cycle slips in the carrier phase data, ionospheric disturbances and loss-of-lock. To accommodate these model biases, the alternative hypotheses are formulated as

$$\mathcal{H}_a : E(\Delta y) = (I_{k-1} \otimes G)\Delta g + (D_k^T s_l \otimes H)b \quad (24.7)$$

where

$$H_{(2n+1) \times q} = \begin{cases} (I_n, 0, 0)^T & \text{(phase loss of lock)} \\ (\delta_j^T, 0, 0)^T & \text{(carrier phase)} \\ (0, \delta_j^T, 0)^T & \text{(pseudo range)} \\ (0, 0, 1)^T & \text{(ionosphere)} \end{cases} \quad (24.8)$$

and

$$s_l_{k \times 1} = \begin{cases} (0, \dots, 0, 1, 0, \dots, 0)^T & \text{(spike)} \\ (0, \dots, 0, 1, 1, \dots, 1)^T & \text{(slip)} \end{cases} \quad (24.9)$$

The n -vector δ_j denotes the unit vector having a 1 as its j th entry.

Stochastic model: With the time-invariant variance matrices of the undifferenced carrier phase and (code) pseudo range observables $\phi(t)$ and $p(t)$ denoted as $Q_{\phi\phi}$ and Q_{pp} , respectively, the dispersion of the two-epoch model (24.4) is assumed to be given as

$$D(y(t, s)) = \text{blockdiag}(2Q_{\phi\phi}, 2Q_{pp}, \sigma_{\Delta, \mathcal{I}}^2) \quad (24.10)$$

where the scalar $\sigma_{\Delta, \mathcal{I}}^2$ denotes the variance of the time-differenced ionospheric delay.

If we assume that the time series of the absolute ionospheric delays can be modelled as a *first-order autoregressive* stochastic process ($\sigma_{\mathcal{I}}^2 \beta^{|t-s|}$, with $0 \leq \beta \leq 1$), the variance of the time-differenced ionospheric delay works out as

$$\sigma_{\Delta, \mathcal{I}}^2 = 2\sigma_{\mathcal{I}}^2(1 - \beta^{|t-s|}) \quad (24.11)$$

For two successive epochs we have $2\sigma_{\mathcal{I}}^2(1 - \beta)$, while for larger time-differences the variance will tend to the white-noise value $2\sigma_{\mathcal{I}}^2$ if $\beta < 1$. Thus $\sigma_{\mathcal{I}}^2$ and β can be used to model the level and smoothness of the noise in the ionospheric delays.

For the measurement precision of the multi-frequency GNSS signals, we assume $Q_{\phi\phi} = \sigma_{\phi}^2 I_{2n}$

Table 24.1 Standard deviations of undifferenced GPS and Galileo observables (Simsky et al., 2006)

	L1	L2	L5	E1	E5a	E5b	E5	E6
Code (cm)	15	15	3.9	6.1	3.9	3.7	0.9	4.4
Phase (mm)	1.0	1.3	1.3	1.0	1.3	1.3	1.3	1.2

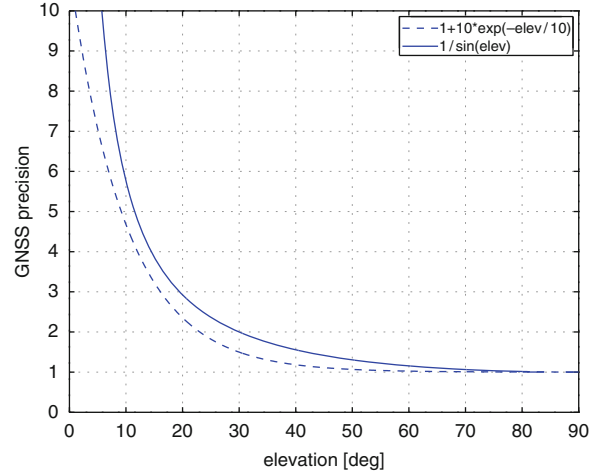


Fig. 24.1 The exponential $1 + 10 \exp(-E/10)$ and the cosecant function $1/\sin(E)$

and $Q_{pp} = \sigma_p^2 I_{2n}$, where we used the values as given by De Wilde et al. (2006), see also De Bakker et al. (2009). These zenith-referenced values are summarized in Table 24.1. To obtain the standard deviations for an arbitrary elevation, these values still need to be multiplied with an elevation dependent function. In practice one often uses an exponential or cosecant function, see Fig. 24.1. For these functions, the function values are between 3 and 4 at 15° elevation and approach the minimum of 1 at 90° elevation.

3 Testing and Reliability

In order to test \mathcal{H}_0 against \mathcal{H}_a , we make use of the *uniformly most powerful invariant* (UMPI) test, see e.g., Arnold (1981), Koch (1999), Teunissen (2006). The UMPI test rejects the null hypothesis \mathcal{H}_0 in favour of the alternative hypothesis \mathcal{H}_a , if

$$T_q = \hat{b}^T Q_{\hat{b}\hat{b}}^{-1} \hat{b} > \chi_{\alpha}^2(q, 0) \quad (24.12)$$

where \hat{b} , with variance matrix $Q_{\hat{b}\hat{b}}$, is the least-squares estimator of b under \mathcal{H}_a , and $\chi_{\alpha}^2(q, 0)$ is the α -level critical value. The UMPI-test statistic T_q is distributed

as $T_q \stackrel{\mathcal{H}_0}{\sim} \chi^2(q, 0)$ and $T_q \stackrel{\mathcal{H}_a}{\sim} \chi^2(q, \lambda)$, respectively, where $\lambda = b^T Q_{\hat{b}\hat{b}}^{-1} b$ is the *noncentrality parameter*.

The power of the test, denoted as γ , is defined as the probability of correctly rejecting \mathcal{H}_0 , thus $\gamma = P[T_q > \chi_\alpha^2(q, 0) | \mathcal{H}_a]$. It depends on q (the dimension of b , a.k.a. degrees of freedom of test), α (level of significance), and through the noncentrality parameter λ , on b (the bias vector). Once q , α and b are given, the power can be computed.

One can however also follow the inverse route. That is, given the power γ , the level of significance α and the dimension q , the noncentrality parameter can be computed, symbolically denoted as $\lambda_0 = \lambda(\alpha, q, \gamma)$. With λ_0 given, one can invert the equation $\lambda_0 = b^T Q_{\hat{b}\hat{b}}^{-1} b$ and obtain

$$\text{MDB} = \sqrt{\frac{\lambda_0}{d^T Q_{\hat{b}\hat{b}}^{-1} d}} d \quad (d = \text{unit vector}) \quad (24.13)$$

This is Baarda's (1968) celebrated *Minimal Detectable Bias* (MDB) vector. The length of the MDB vector is the smallest size of bias vector that can be found with probability γ in the direction d with test (24.12). By letting d vary over the unit sphere in \mathbb{R}^q one obtains the whole range of MDBs that can be detected with probability γ with test (24.12). The MDB can be computed once λ_0 and $Q_{\hat{b}\hat{b}}$ are known. The value of λ_0 depends on q , α and γ . For later use, we have shown the dependence in Fig. 24.2 of $\sqrt{\lambda_0}$ on γ for different values of q and α .

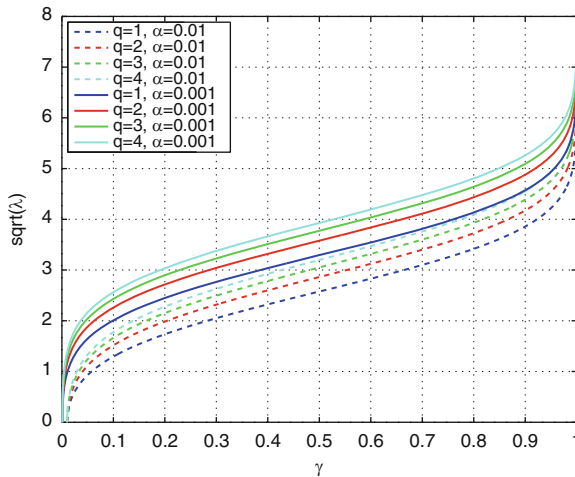


Fig. 24.2 Square root of noncentrality parameter λ_0 as function of power γ for degrees of freedom $q = 1, 2, 3, 4$ and levels of significance $\alpha = 0.01, 0.001$

We now present an analytical expression for the MDB of the single-receiver carrier-phase slip. First we consider the single-frequency receiver, then the multi-frequency GNSS receiver.

4 Single Frequency Receiver MDB-Slip

The two-epoch, single-frequency receiver MDB for a carrier-phase slip can be shown to read as

$$\text{MDB}_{\phi_j} = \sqrt{2(\sigma_{\phi_j}^2 + \sigma_{p_j}^2 + 4\mu_j^2 \sigma_I^2)} \lambda_0 \quad (24.14)$$

where $\sigma_I = \sigma_{\mathcal{S}} \sqrt{1 - \beta^{|t-s|}}$. This expression clearly shows how the detectability is affected by the measurement precision ($\sigma_{\phi_j}, \sigma_{p_j}$), the signal frequency (μ_j), and the time-smoothness of the ionosphere (σ_I).

In Fig. 24.3 we show the single-frequency phase-slip MDB ϕ_j s for GPS and Galileo as function of σ_I . For Fig. 24.3 we used the frequencies of Tables 24.2 and 24.3, and the standard deviations of Table 24.1. The figure clearly shows the effects of (code) measurement precision and frequency. For small values of σ_I , the effect of (code) measurement precision dominates, while for larger values, the frequency effect starts to be felt.

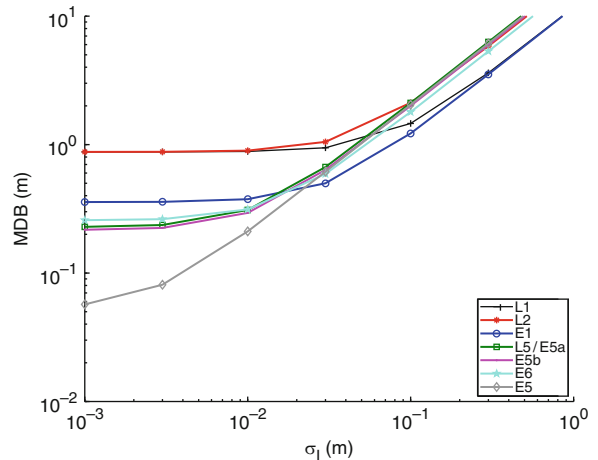


Fig. 24.3 Single-frequency phase-slip MDBs as function of $\sigma_I = \sigma_{\mathcal{S}} \sqrt{1 - \beta^{|t-s|}}$. The MDBs are shown for the GPS frequencies L1, L2, and L5, and the Galileo frequencies E1, E5, E5a, E5b, E6 (NB: $k = 2$, $\alpha = 0.001$, $\gamma = 0.80$ and $\mathcal{S}(t)$ is defined w.r.t. L1 frequency)

Table 24.2 GPS frequencies and wave lengths

	L1	L2	L5
Frequency (MHz)	1575.42	1227.60	1176.45
Wave length (cm)	19.0	24.4	25.5

Table 24.3 Galileo frequencies and wave lengths

	E1	E5a	E5b	E5	E6
Freq (MHz)	1575.420	1176.450	1207.140	1191.795	1278.750
λ (cm)	19.0	25.5	24.8	25.2	23.4

Since all MDBs, except the E5-MDB, are larger than 20 cm, one can not expect a single-frequency receiver to perform well on these frequencies as far as cycle slip detection is concerned. Even for those that have their MDB around their wave length – like L5, E5a and E5b – one should keep in mind that these values will become larger for lower elevations.

Cycle slip detection on the E5 frequency does however have a good chance of performing well. The zenith-referenced E5-MDB is about 8 cm for $\sigma_I = 3$ mm. Since this value will have to be multiplied by about 3 to get the 20° elevation MDB, the result still stays below the E5 wave length of 25.2 cm.

For the other frequencies, single-frequency cycle slip detection will be difficult when using the single-receiver, single-satellite geometry-free model.

5 Multi Frequency Receiver MDB-Slips

The two-epoch, multi-frequency carrier phase slip MDB can be shown to read as

$$MDB_{\phi_j} = \sigma_{\phi} \sqrt{\left(\frac{2}{1 - \frac{1}{n^*}}\right) \lambda_0} \quad (24.15)$$

where

$$\frac{1}{n^*} = \frac{1}{n} \frac{1}{1 + \varepsilon} \left(1 + \frac{(\mu_j - \frac{1-\varepsilon}{1+\varepsilon} \bar{\mu})^2}{\frac{1}{n} \sum_{i=1}^n \mu_i^2 - \left(\frac{1-\varepsilon}{1+\varepsilon}\right)^2 \bar{\mu}^2 + \frac{\sigma_{\phi}^2 / \sigma_I^2}{n(1+\varepsilon)}} \right) \quad (24.16)$$

with the phase-code variance ratio $\varepsilon = \sigma_{\phi}^2 / \sigma_p^2$ and the average $\bar{\mu} = \frac{1}{n} \sum_{j=1}^n \mu_j$.

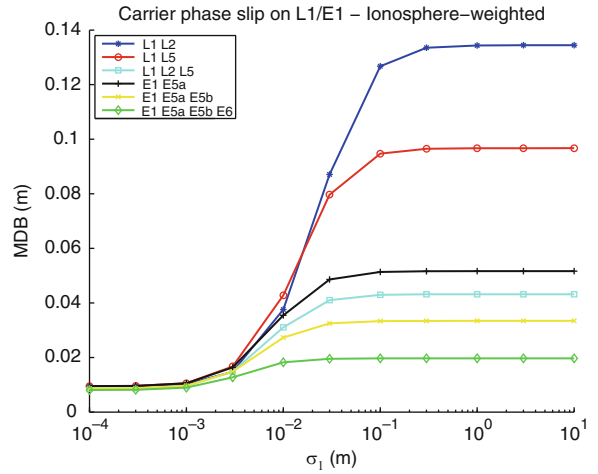


Fig. 24.4 Multi-frequency phase-slip MDBs as functie of $\sigma_I = \sigma_{\mathcal{I}} \sqrt{1 - \beta^{|t-s|}}$. The MDBs are shown for dual- and triple-frequency GPS, and for dual- triple- and quadruple-frequency Galileo. (NB: $k = 2$, $\alpha = 0.001$, $\gamma = 0.80$ and $\mathcal{I}(t)$ is defined w.r.t. L1 frequency)

The dual-, triple- and quadruple-frequency MDB phase-slips for GPS and Galileo are shown in Fig. 24.4. The quadruple-frequency Galileo-case performs best, while the dual-frequency GPS-case performs poorest. In all cases however, the MDBs are below the 1-cycle level, even below the 5 cm if $\sigma_I \leq 1$ cm. Thus single-receiver, multi-frequency cycle slip detection will be possible for such ionospheric conditions. For the more extreme case that σ_I is several cm, GPS dual-frequency (e.g. $L_1 L_2, L_1 L_5$) cycle slip detection will become problematic for lower elevations.

Acknowledgements The research of the first author has been supported by an Australian Research Council Federation Fellowship (project number FF0883188).

References

Arnold SF (1981) The theory of linear models and multivariate analysis. Wiley, New York
 Baarda W (1968) A testing procedure for use in geodetic networks. Netherlands geodetic commission, Publ Geodes, New Series, 2(5)
 De Bakker PF, van der Marel H, Tiberius CCJM(2009) Geometry-free undifferenced, single and double differenced analysis of single frequency GPS, EGNOS and GIOVE-A/B measurements. GPS Solut 13(4): 305–314

- Hofmann-Wellenhoff B, Lichtenegger H (2001) Global positioning system: theory and practice, 5th edn. Springer, Berlin
- De Jong K (2000) Minimal detectable biases of cross-correlated GPS observations. *GPS Solutions* 3:12–18.
- De Jong K, Teunissen PJG (2000) Minimal detectable biases of GPS observations for a weighted ionosphere. *Earth, Planets and Space* 52:857–862
- Koch KR (1999) Parameter estimation and hypothesis testing in linear models, 2nd edn. Springer, Berlin
- Leick A (2003) GPS satellite surveying, 3rd edn. Wiley, New York
- Misra P, Enge P (2001) Global positioning system: signals, measurements, and performance. Ganga-Jamuna Press, Lincoln MA
- Teunissen PJG (1998) Minimal detectable biases of GPS data. *J Geodes* 72:236–244
- Teunissen PJG (2006) Testing theory; an introduction, 2nd edn. Delft VSSD
- Teunissen PJG and Kleusberg A (eds) (1998) GPS for geodesy, 2nd enlarged edn., Springer, Berlin
- De Wilde W, Wilms F, Simsky A, Sleewaegen J (2006). Early performance results for new Galileo and GPS signals-in-space. In: Proceedings of ENC GNSS, 2006. Manchester